NJC

Accepted Manuscript

This is an *Accepted Manuscript*, which has been through the Royal Society of Chemistry peer review process and has been accepted for publication.

Accepted Manuscripts are published online shortly after acceptance, before technical editing, formatting and proof reading. Using this free service, authors can make their results available to the community, in citable form, before we publish the edited article. We will replace this *Accepted Manuscript* with the edited and formatted *Advance Article* as soon as it is available.

You can find more information about *Accepted Manuscripts* in the Information for Authors.

Please note that technical editing may introduce minor changes to the text and/or graphics, which may alter content. The journal's standard Terms & Conditions and the Ethical guidelines still apply. In no event shall the Royal Society of Chemistry be held responsible for any errors or omissions in this *Accepted Manuscript* or any consequences arising from the use of any information it contains.

ROYAL SOCIETY OF CHEMISTRY

www.rsc.org/njc

Leaching kinetics of cerussite using a new complexation reaction reagent

Dandan Wu[a] ·Shuming Wen[a]·Jiushuai Deng[a*]

[a] *State Key Laboratory of Complex Nonferrous Metal Resources Clean Utilization, Faculty of Land Resource Engineering, Kunming University of Science and Technology, Kunming 650093, PR China*

Abstract: In this paper, an attractive organic complexation reaction reagent with lead ions was developed for lead extraction from cerussite. The leaching kinetics of cerussite was investigated using 5-sulfosalicylic acid solution as lixiviant. The effects of several experimental parameters on the leaching of cerussite were investigated, and a kinetic model was developed to represent these relationships. The leaching process was controlled by a mixed kinetic model. Results showed that the leaching rate of cerussite increased with increased stirring speed, temperature, and concentration, as well as decreased particle size. The activation energy was found to be 37.07 kJ/mol. The rate of reaction based on the mixed kinetic model-controlled process could be expressed as $[1-(1-x)^{1/3}]^2 = [k_0(\mathrm{SS})^{6.852}(r_0)^{-1.943}(C)^{2.042}\exp(-37.07/RT)]t$. X-ray diffraction and scanning electron microscopy/energy-dispersive X-ray spectroscopy analyses indicated that a new solid reaction product may be formed.

Keywords: leaching; kinetics; cerussite; 5-sulfosalicylic acid; complexation reaction

* Corresponding author. *E-mail address:* dengshuai689@163.com (Jiushuai Deng)

1. Introduction

Natural lead enrichment most frequently occurs as the mineral galena (PbS). Some other oxidation products of lead ores include anglesite ($PbSO_4$) and cerussite ($PbCO_3$) [1]. Cerussite occurs in the weathered zone of lead sulphide ore deposits, most commonly as an alteration product of galena. Cerussite crystallizes in the orthorhombic system and is isomorphous with aragonite.

To date, only pyrometallurgical smelting methods have been commercialized for lead extraction from its sulfide ores and some other secondary lead sources. Thus, alternative processes for the hydrometallurgical treatment of lead-bearing ores are receiving significant interest because of the environmental impact of the conventional pyrometallurgical smelting route and the rising demand for lead metal. Accordingly, the recovery of lead from oxidized resources with hydrometallurgical methods is proposed and has become a research hotspot. [1]

Studies on the dissolution of lead-bearing minerals in acid solutions are few. The dissolution kinetics of a Nigerian galena ore in hydrochloric acid solution has been discussed by Baba and Adekola. [2] They described the influence of acid concentration, temperature, particle size, stirring speed, and solid/liquid ratio on the dissolution extent. Their results show that 94.8% of galena is dissolved by 8.06 M HCl at 80 °C within 120 min with an initial solid/liquid ratio of 10 g/L. The corresponding activation energy E_a was calculated to be 38.74 kJ/mol. Gutiérrez and Lapidus [3] investigated the thermodynamics and kinetics of anglesite leaching in citrate solutions.

Solution pH and pulp density are found to profoundly affect lead extraction. Their thermodynamic analysis suggests that lead solubility in citrate is maximized at pH values near 7, as corroborated by leaching tests. Limited solubility is found to severely hamper the leaching rate at high pulp densities. A hydro-electrometallurgical process of treating cerussite concentrate by methanesulfonic acid (MSA) has also been proposed. [1] Cerussite concentrate is first leached with MSA, and then several parameters (temperature, stirring speed, acid concentration, particle size, and solid/liquid ratio) are considered.

5-Sulfosalicylic acid (SSA) belongs to the aromatic oxyacid family [4] and is widely used in many fields because of its better water solubility than other derivatives of salicylic acid. [5] SSA is an important chelating agent that can form coordinate bonds with many transient metal ions. Thus, SSA is often chosen as an adsorbing material and masking agent of metal ions. [6]

SSA easily forms ligands with lead ions, and potential complexation reactions could occur in an aqueous solution. Consequently, this complexation reaction has gained extensive research interest. Furthermore, the functional groups of SSA could be partially or completely deprotonated to obtain an aqueous acidic solution, [7] so that cerussite could be dissolved in the acidic environment. Based on its ionization and complexation properties, SSA can be used as a potential leaching reagent for oxide ores.

To the best of our knowledge, no study on the leaching kinetics of cerussite in SSA solutions has been conducted. Accordingly, this study aimed to investigate the

leaching kinetics of cerussite using SSA as lixiviant. The effects of several parameters, including stirring speed, temperature, particle size, and acid concentration, on lead extraction were investigated, and leaching conditions were optimized. A mixed kinetic control model was found to suitably explain the relationship between reaction time and fraction of lead leached. Finally, the apparent activation energy of the process was determined.

2. Material and methods

2.1. Materials

Pure cerussite samples were obtained from Yunnan Province, China. The ore samples were crushed, ground, and passed through standard test sieves to obtain desired particle size fractions. Mineralogical analysis of the cerussite samples was conducted by X-ray diffraction (XRD) using a Rigaku D/max 2550VB+ 18 kW powder diffractometer equipped with a Cu/K_α X-ray source operated at 40 kV and 40 mA. The morphological features of cerussite and its leaching residues were studied using a scanning electron microscopy (SEM) (Hitachi S-3400N) system. Fig. 1(a) shows the results of XRD analysis, which indicated that the samples consisted of cerussite, quartz, and calcium carbonate. The results of chemical analysis on cerussite are presented in Table 1.

Table 1 Chemical composition of pure cerussite samples.

Element	Pb	Zn	CaO	Al_2O_3	SiO_2
Content (%)	57.96	0.056	3.43	1.53	18.90

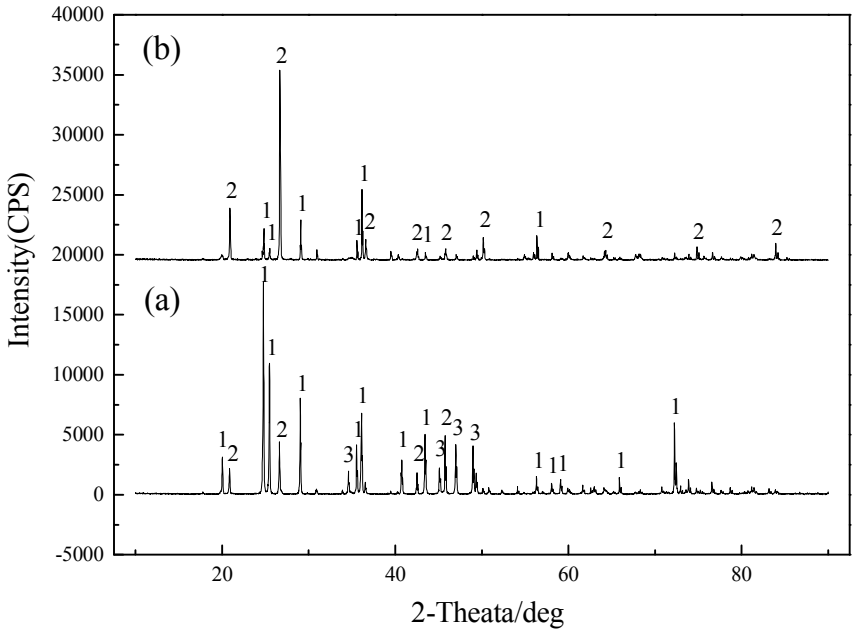

Fig.1. X-ray diffraction patterns of cerussite samples (a) before and (b) after leaching.

2.2. Experimental procedure

Leaching was carried out in a 1000 mL three-necked flask batch reactor heated with a thermostat to maintain the contents at a constant temperature during reaction. The reactor was further equipped with a digital controlled mechanical stirrer for stirring, a thermometer for temperature control, and a condenser to prevent evaporation loss. In a typical experiment, 5 g of solid was added to 1000 mL of freshly prepared SSA solutions with different concentrations. From this mixture, 5 mL samples were accurately withdrawn periodically for analysis. Lead extraction rate was determined by analyzing the concentration of lead in the solution by inductively coupled plasma–atomic emission spectroscopy. At the end of the reaction, the residue was filtered and washed with de-ionized water. The residue was air dried and then identified by XRD and SEM. The results are shown in Figs. 1 and 3, respectively.

The conversion fraction of cerussite was calculated as follows: x = mass of lead passing to the solution/mass of lead in the ore sample. In the tests, the effect of one parameter was investigated by keeping the values of the other parameters (marked with asterisks in Table 2 constant. The leaching data obtained were plotted as a function of conversion fraction x versus reaction time t.

Table 2 Leaching parameters and ranges used in leaching experiments.

Parameter	Value
Concentration (mol/L)	0.1, 0.15, 0.2, 0.25*, 0.3
Reaction temperature (°C)	20, 30, 40, 50*, 60
Stirring speed (rpm)	200, 400, 600, 800*, 1000
Average particle size (μm)	320, 200, 124, 80*, 50

*These parameters were kept constant.

3. Results and discussion

3.1. Leaching reactions

SSA is a strong organic acid with three functional groups, namely, –OH, –COOH, and $–SO_3H$, [7] Fig. 2 shows the five structure types of SSA. Among them, all three hydrogen occur in the metal complexes of lead or other metals. SSA in aqueous medium follows the reaction:

$$C_7H_6O_6S \rightarrow C_7H_3O_6S^{3-}{}_{(aq)} + 3H^{+}{}_{(aq)} \quad (1)$$ or

$$C_7H_6O_6S + 3H_2O_{(aq)} \rightarrow C_7H_3O_6S^{3-}{}_{(aq)} + 3H_3O^{+}{}_{(aq)} \quad (2)$$

When cerussite is added to SSA solution, the reaction during dissolution is expected to be as follows:

$$PbCO_3 + 2H^{+}{}_{(aq)} \rightarrow Pb^{2+}{}_{(aq)} + H_2O_{(aq)} + CO_{2(g)} \quad (3)$$

Consequently, the overall leaching reaction can be written as follows:

$$3PbCO_3 + 2C_7H_6O_6S \rightarrow 3Pb^{2+}_{(aq)} + 2C_7H_3O_6S^{3-}_{(aq)} + 3H_2O_{(aq)} + 3CO_{2(g)} \quad (4)$$

A stable complex could reportedly be formed by the complexation reaction between SSA and lead ions, [5] whereas the following reaction may occur in an aqueous solution:

$$Pb^{2+}_{(aq)} + 2SSA_{(s)} \leftrightarrows Pb(SSA)_2{}^{2+}_{(aq)} \quad (5)$$

On one hand, SSA could provide an acidic environment; on the other hand, SSA could serve as a complexation reaction reagent with lead ions. Thus, SSA could exert a new leaching effect on cerussite.

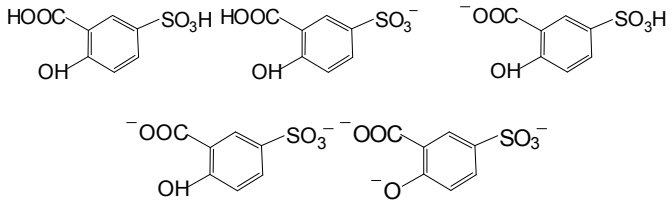

Fig. 2. Five structure types of SSA.

3.2. XRD and morphology of leaching residues

The XRD patterns of cerussite samples were measured to understand their dissolution behaviors in SSA solution. Fig. 1(a) shows that before dissolution, the samples consisted of cerussite, quartz, and calcium carbonate. Meanwhile, after dissolution, the XRD patterns in Fig. 1(b) exhibited differences with the patterns before reaction.

To investigate the change in product morphology after leaching, raw ore and residues were observed under a scanning electron microscope. Before dissolution (Fig. 3(a)), the white blocky parts and black parts were determined to be cerussite and black gangue minerals, respectively. EDS analysis with statistical sampling (Table 3) revealed that this main contents were Pb, C, O, Si, Al, and Fe. From the Fig. 3(b) it

can be seen that white blocks of cerussite and black blocks of quartz after dissolution. After a period of complexation reaction, lead ions and SSA are likely to be formed a white blocky complex. Results of EDS analysis showed that almost no lead was contained in the black residue (Fig. 4(b-2)), which had only 37.88% O and 62.12% Si.

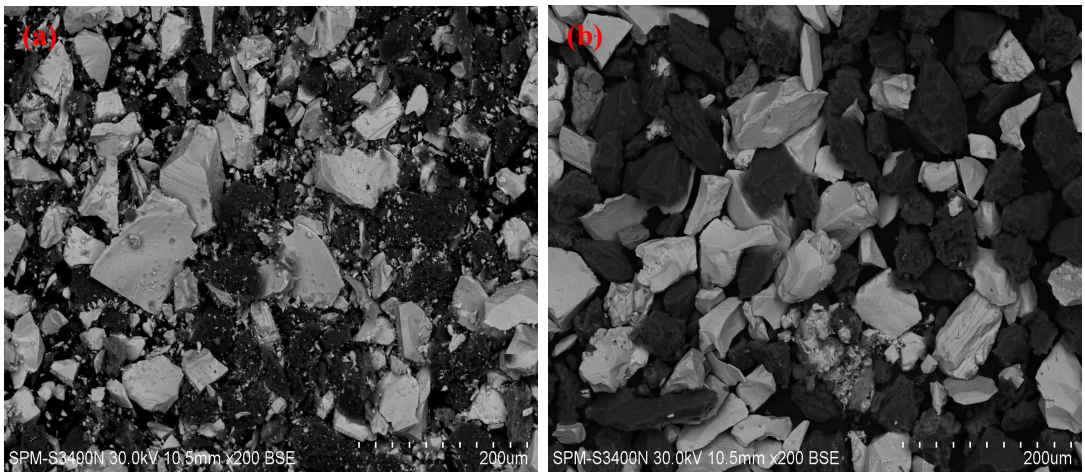

Fig. 3. Scanning electron micrographs of cerussite samples: (a) before SSA and (b) after SSA dissolution.

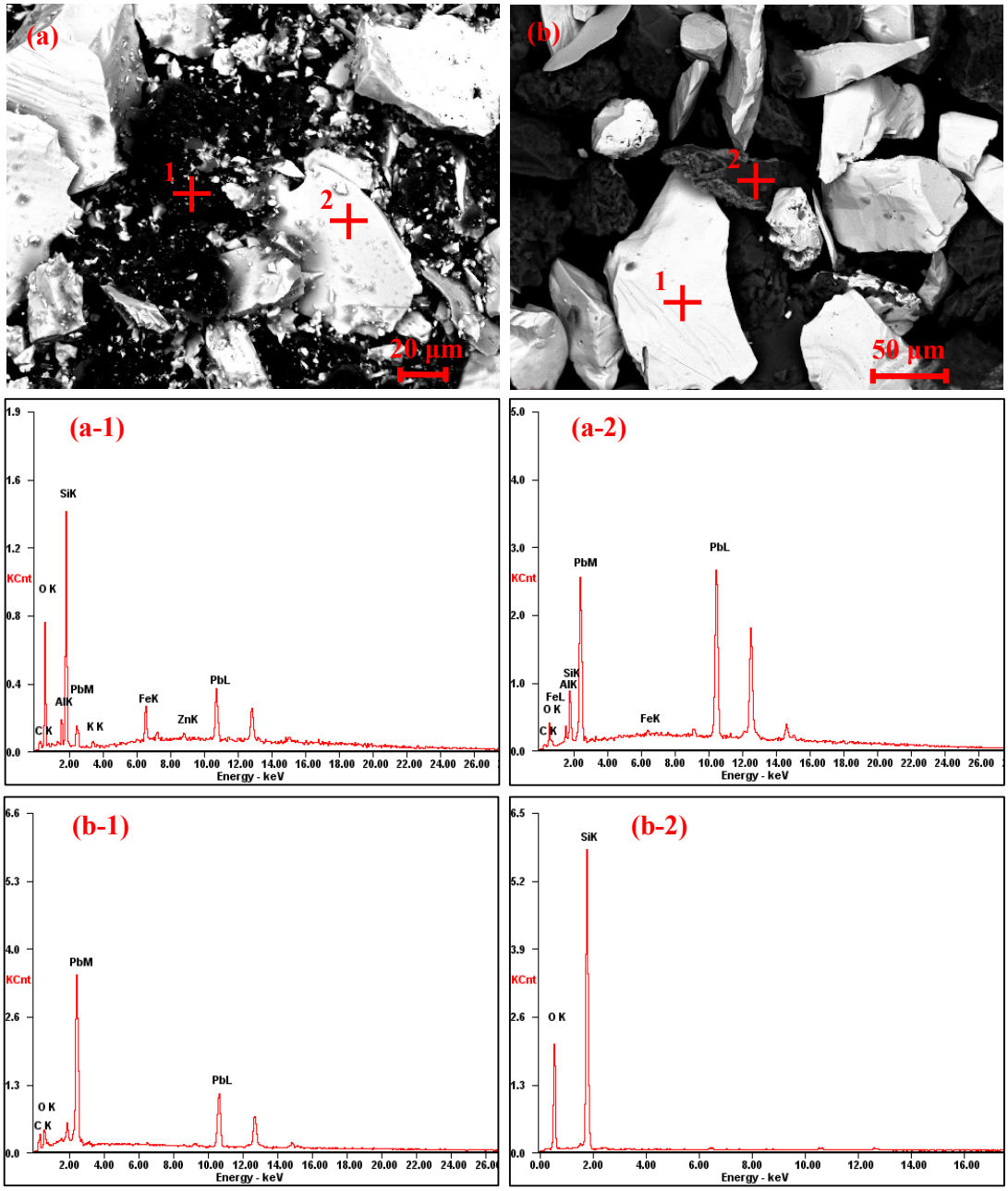

Fig. 4. SEM/EDS data of cerussite samples: (a) before and (b) after dissolution.

Table 3 EDS spectrum element content in semi-quantitative analysis results.

	Element	*Concentration (%)*	
		Wt.	***At.***
(a-1)	*CK*	00.70	16.73
	OK	37.60	61.33
	AlK	02.19	02.12

	SiK	14.59	13.56
	K K	00.46	00.31
	FeK	02.89	01.35
	ZnK	00.93	00.37
	PbL	33.65	04.24
(a-2)	*CK*	03.07	19.85
	OK	07.41	35.96
	AlK	01.09	03.13
	SiK	03.14	08.68
	FeK	00.39	00.55
	PbL	84.90	31.83
(b-1)	*CK*	17.00	50.87
	OK	16.75	37.64
	PbL	66.25	11.49
(b-2)	*OK*	62.12	74.22
	SiK	37.88	25.78

3.3. Effect of SSA concentration

A number of tests each lasting for 30 min were conducted to determine the effects of SSA concentration on lead extraction. The experiments were carried out at five different SSA concentrations within the range of 0.1 mol/L to 0.3 mol/L. While conducting these tests, the values of other experimental parameters were kept constant at 50 °C, 800 rpm, and 80 μm. Results (Fig. 5) showed that the leaching rate of cerussite considerably increased with increased SSA concentration. At 0.1 mol/L SSA concentration, 49.37% lead was leached; at 0.3 mol/L, 96.11% of lead was extracted. Thus, the extent of lead extraction from cerussite clearly increased with increased lixiviant concentration.

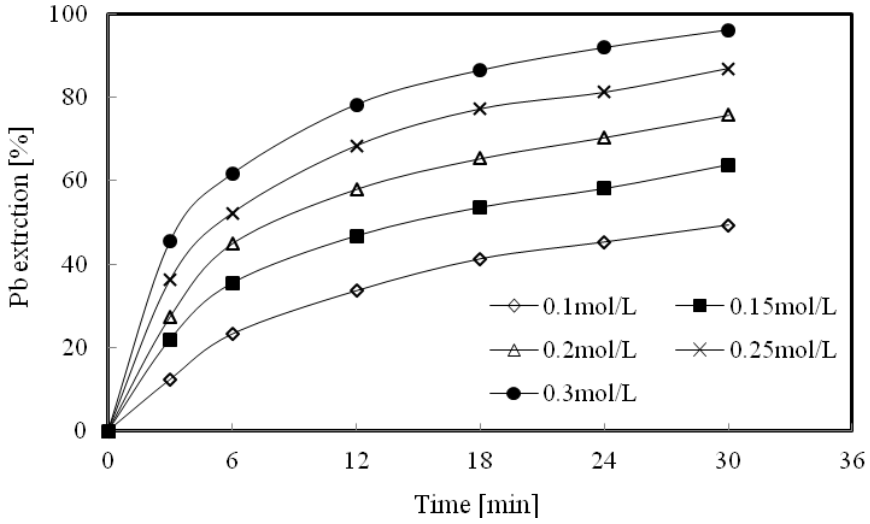

Fig. 5. Effect of SSA concentration on cerussite dissolution.

3.4. Effect of reaction temperature

Reaction temperature is a very important factor affecting dissolution kinetics. The effect of this parameter was examined at 20, 30, 40, 50, and 60 °C. During the experiments, SSA concentration, stirring speed, and average particle size were kept constant at 0.25 mol/L, 800 rpm, and 80 μm, respectively. The leaching curves are shown in Fig. 6. The leaching rate was found to increase with increased reaction temperature. Thus, reaction temperature significantly affected lead dissolution. After 30 min of dissolution, the amounts of lead extracted from cerussite were 58.41% and 95.52% at 20 and 60 °C, respectively.

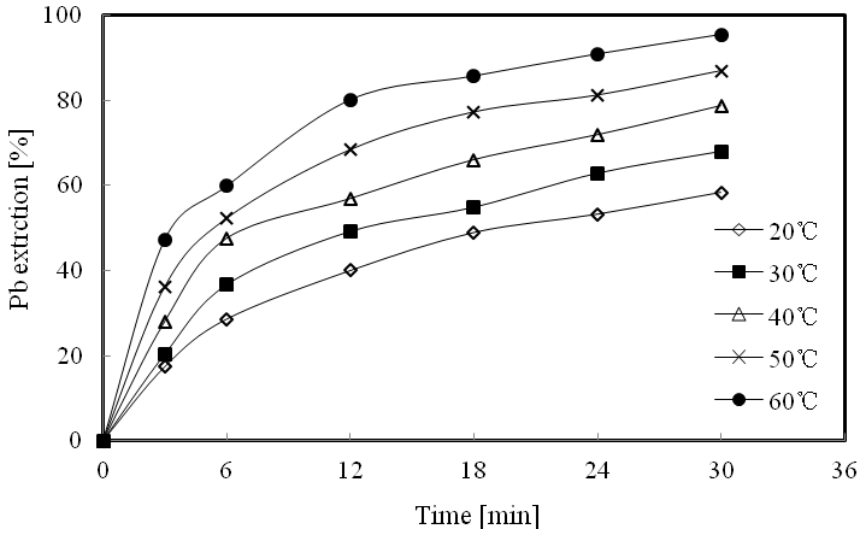

Fig. 6. Effect of temperature on cerussite dissolution.

3.5. Effect of stirring speed

As shown in Fig. 7, the effect of stirring speed on cerussite leaching was investigated by varying this parameter (200, 400, 600, 800, and 1000 rpm) while keeping constant SSA concentration, reaction temperature, and average particle size at 0.25 mol/L, 50 ℃, and 80 μm, respectively. A remarkable effect of stirring speed on lead leaching rate was experimentally proved. When the stirring speed was 200 rpm, the lead leaching rate was 37.97%; when the stirring speed was 1000 rpm, the rate was 97.18%, i.e., cerussite was almost completely dissolved. Therefore, stirring speed significantly affected cerussite dissolution.

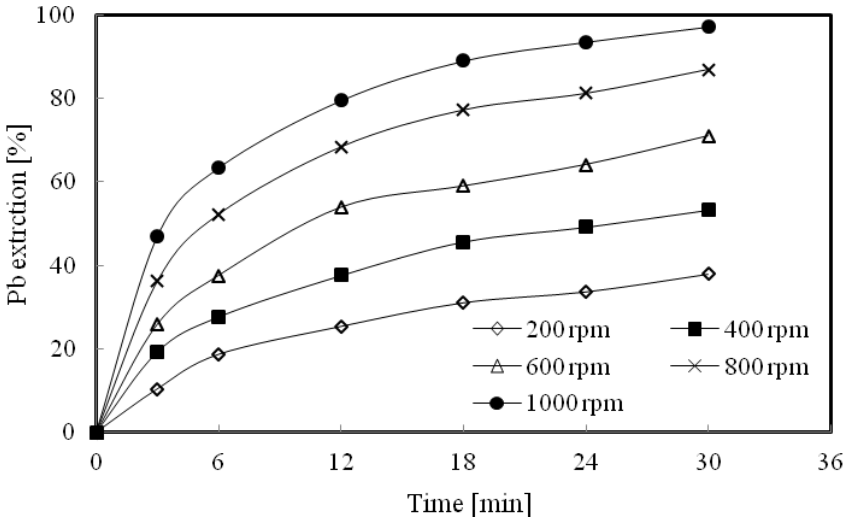

Fig. 7. Effect of stirring speed on cerussite dissolution.

3.6. Effect of average particle size

The effect of average particle size on leaching was studied by varying this parameter (320, 200, 124, 80, and 50 μm) while keeping constant SSA concentration, reaction temperature, and stirring speed at 0.25 mol/L, 50 °C, and 800 rpm, respectively. Results (Fig. 8) indicated that smaller particle sizes resulted in faster lead dissolution. With decreased particle size, the contact area between particles and fluid increased. The lead extraction rates obtained after 30 min of reaction were 33.87% at 320 μm and 98.32% at 50 μm average particle size. Therefore, the average particle size significantly affected lead dissolution.

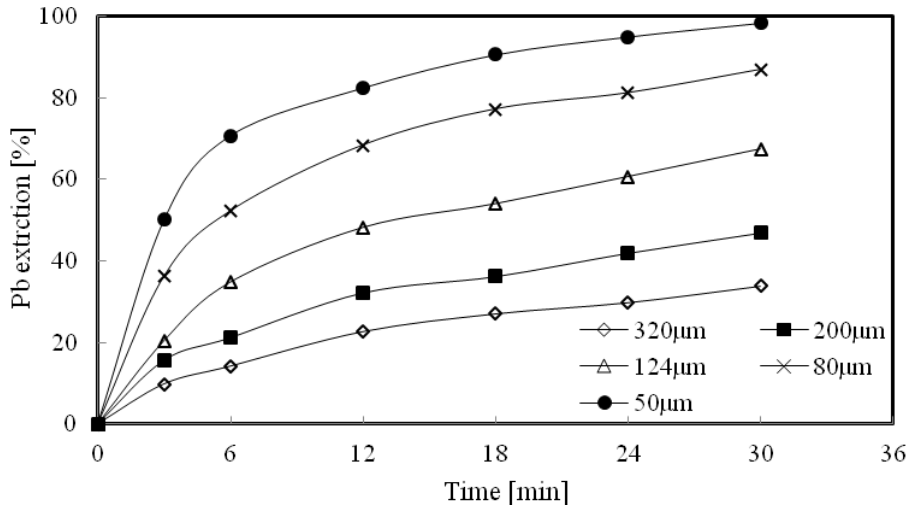

Fig. 8. Effect of particle size on cerussite dissolution.

3.7. Kinetic study

The leaching reaction of mineral particles with a reagent (a solid–fluid reaction) is expressed as:

$$aA_{\text{fluid}} + bB_{\text{solid}} \rightarrow \text{product} \quad (6)$$

where a, b, A, and B represent the stoichiometric coefficient, fluid reactant, and solid undergoing dissolution, respectively. The kinetics of leaching reactions is often described by the shrinking core model, wherein a reaction between solid and fluid reactants occurs on the outer surface of the solid. The solid reactant is initially surrounded by a fluid film through which mass transfer occurs between the solid and the bulk fluid. As the reaction proceeds, the unreacted core of the solid shrinks toward the solid center, and a porous product layer forms around the unreacted core [8-11].

If the leaching rate is controlled by diffusion through a liquid film, the integrated rate equation is as follows:

$$x = k_l t \quad (7)$$

If the reaction is controlled by a surface chemical reaction, the integrated rate equation of this step is written as follows:

$$1-(1-x)^{1/3}=k_r t \quad (8),$$

If the reaction rate is controlled by diffusion through a product layer, the integrated rate equation is as follows:

$$1-3(1-x)^{2/3}+2(1-x)=k_d t \quad (9)$$

where x is the conversion fraction of solid particles, k_l is the apparent rate constant for diffusion through the fluid film, k_r is the apparent rate constant for the surface chemical reaction, k_d is the apparent rate constant for diffusion through the product layer, and t is the reaction time.

Generally, the kinetics of any leaching reaction fits one of the above models. In addition to these models, the Jander equation is a mixed kinetic model can be used to determine the rate expressions of leaching reactions. The rate equations for the mixed kinetic models are given in the literature, which is based on diffusion-controlled mechanisms. [12] The theory is based on a process proceeded by instantaneous surface nucleation and the diffusion-controlled process.

To determine the kinetic parameters and rate-controlling step of cerussite dissolution in SSA solutions, the experimental data obtained in the leaching step were analyzed based on the shrinking core model using the rate expression given in Equations (7) to (9) and the mixed kinetic models introduced in literature. Among the mixed kinetic models applied to the leaching data, the following model could be more suitable for demonstrating the kinetics of this leaching system.

$$[1-(1-x)^{1/3}]^2 = k_m t \quad (10),$$

where, k_m is the apparent rate constant for the mixed kinetic model.

The apparent rate constants obtained from the plots and the correlation coefficients for each experimental parameter are provided in Table 4. Low regression coefficients were found for film diffusion, surface chemical reaction, and diffusion through product layer models, indicating that none of these processes represented the rate-controlling step. The larger and largest regression coefficients were obtained from the diffusion through product layer model and the mixed kinetic model, respectively, indicating that the diffusion through product layer model and the mixed kinetic model were the rate-controlling step in this dissolution system.

To test the validity of the model in Eq. (10), its left side was plotted versus time for reaction temperature, stirring speed, particle size, and solution concentration. The resulting graphs are shown in Figs. 9–12. Results showed that the kinetic model in Eq. (10) appropriately representated the dissolution process of cerussite. The activation energy of this leaching process was found from the Arrhenius equation, and the Arrhenius plot is shown in Fig. 13. The activation energy of this leaching reaction was calculated to be E = 37.07 kJ/mol.

To test the validity of $1–3(1–x)^{2/3}+2(1–x)$, $1–3(1–x)^{2/3}+2(1–x)$ was plotted versus time for reaction temperature, stirring speed, particle size, and solution concentration. As can be seen from the Table 4 results, diffusion through product layer model has large regression coefficients (R^2 >0.97). Fig. 17 shows the Arrhenius plot of the dissolution process in the kinetic model given in Equation (9). Calculations yielded

E=31.15 kJ/mol. This value is inconsistent with the reaction rate, which was controlled by diffusion through a product layer. These results show that the mixed kinetic model can accurately represent the leaching process.

The equation representing the kinetics of the leaching process can be expressed as

$$[1-(1-x)^{1/3}]^2 = [k_0(\mathrm{SS})^{\alpha}(r_0)^{\beta}.(C)^{\gamma}\exp(-E/RT)]t \quad (11)$$

where SS, r_0, C, E, R, and T are stirring speed, particle size, concentration, activation energy, universal gas constant, and temperature, respectively. The constants α, β, and γ are reaction orders for the related parameters, and k_0 is the frequency or pre-exponential factor.

The constants α, β, and γ were determined to have values of 6.852, −1.943, and 2.042, respectively (Figs. 14–16, respectively). Thus, the leaching kinetics of cerussite can be described by Eq. (11).

$$[1-(1-x)^{1/3}]^2 = [k_0(\mathrm{SS})^{6.852}(r_0)^{-1.943}(C)^{2.042}\exp(-37.07/RT)]t \quad (12)$$

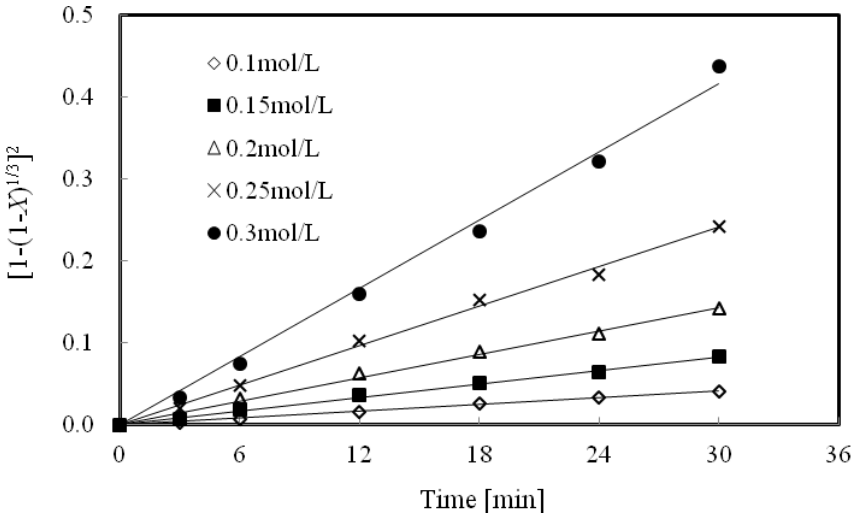

Fig. 9. Plot of $[1-(1-x)^{1/3}]^2$ versus t at various SSA concentrations.

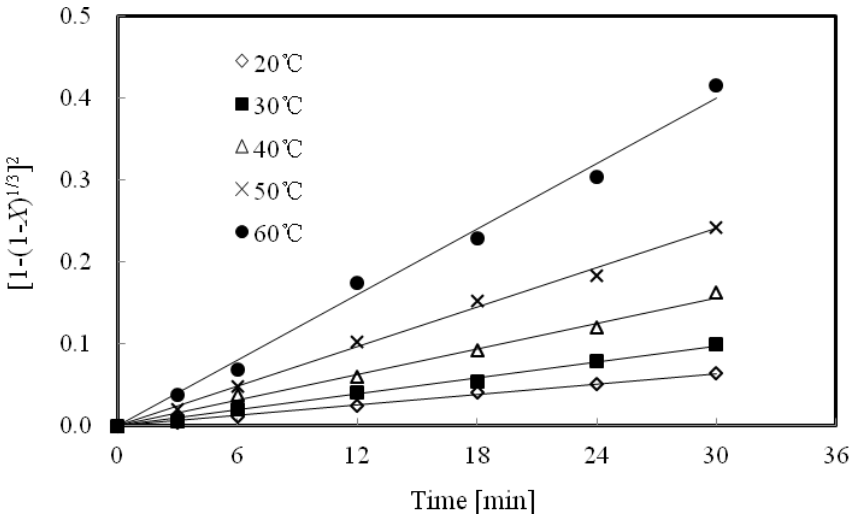

Fig. 10. Plot of $[1-(1-x)^{1/3}]^2$ versus t at various temperatures.

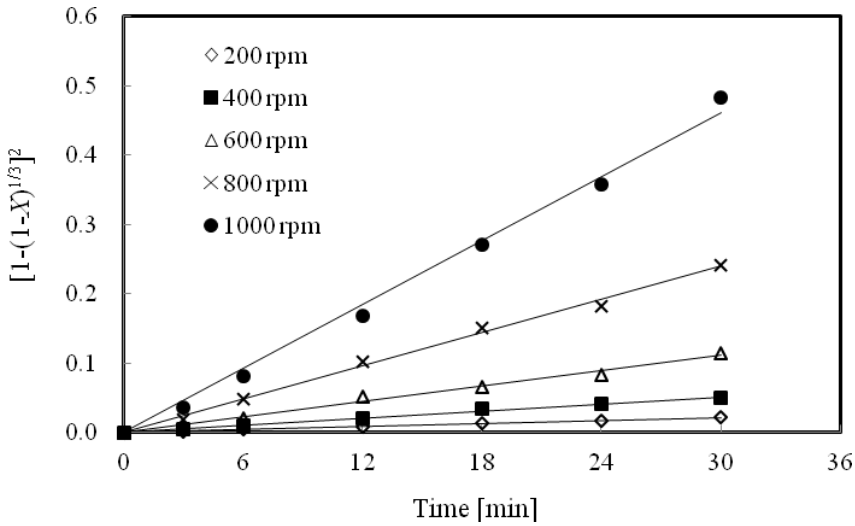

Fig. 11. Plot of $[1-(1-x)^{1/3}]^2$ versus t at various stirring speeds.

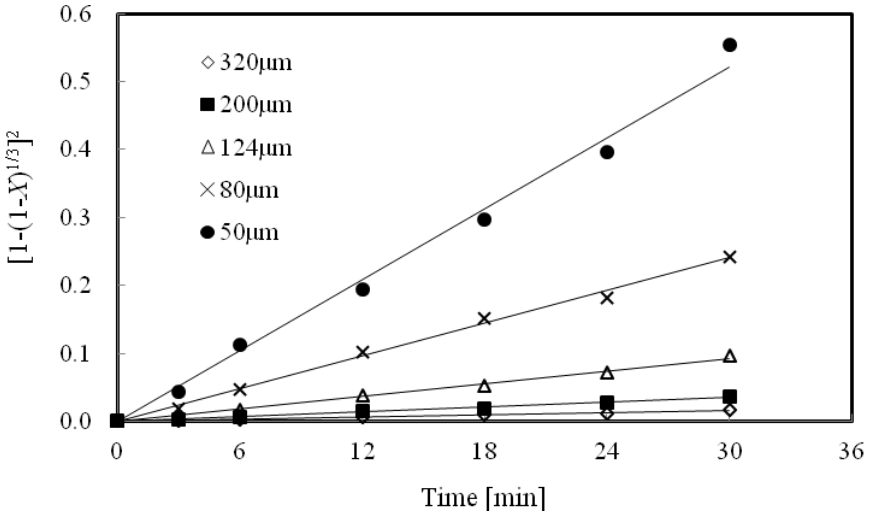

Fig. 12. Plot of $[1-(1-x)^{1/3}]^2$ versus t for various particle sizes.

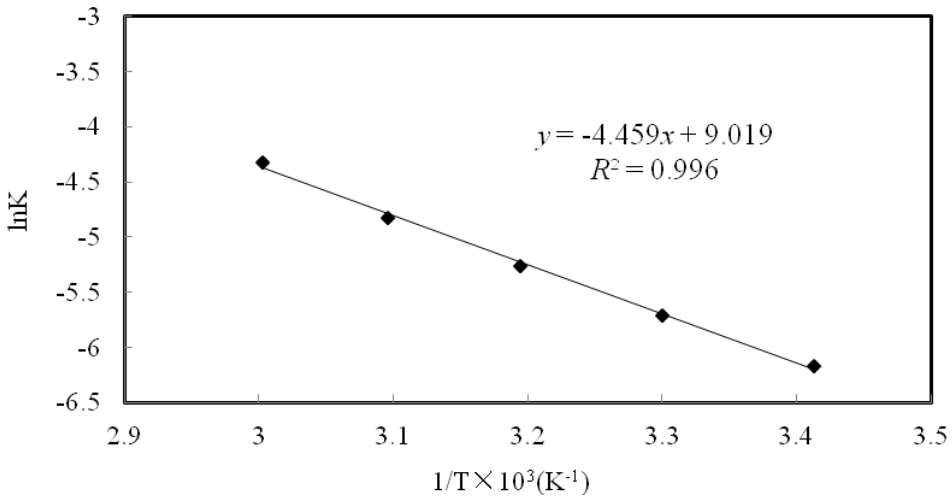

Fig. 13. Arrhenius plot of cerussite dissolution.

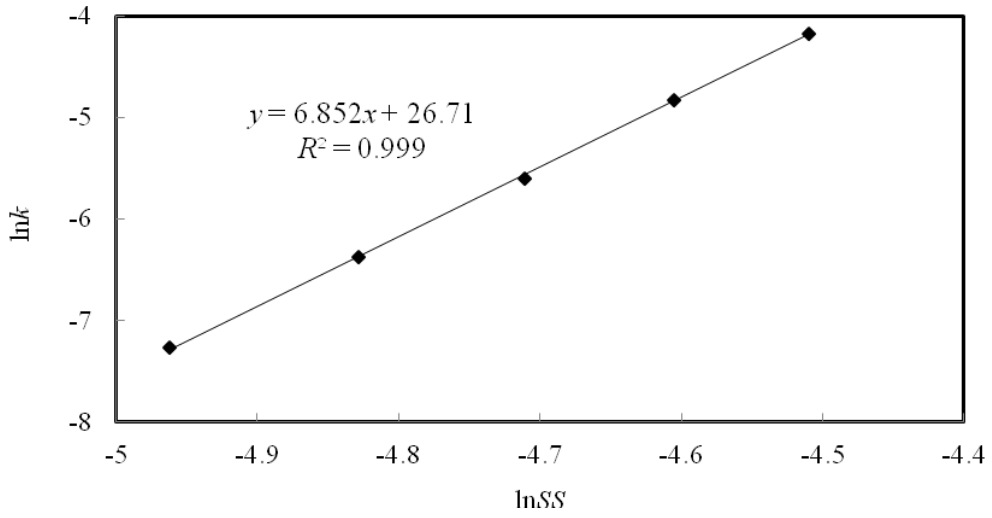

Fig. 14. Plot of ln *k* versus stirring speed.

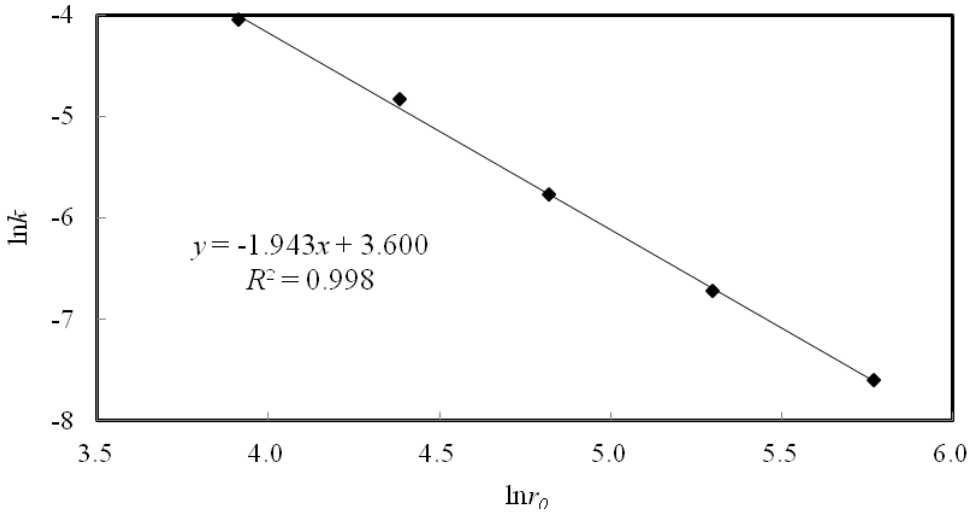

Fig. 15. Plot of ln *k* versus particle size.

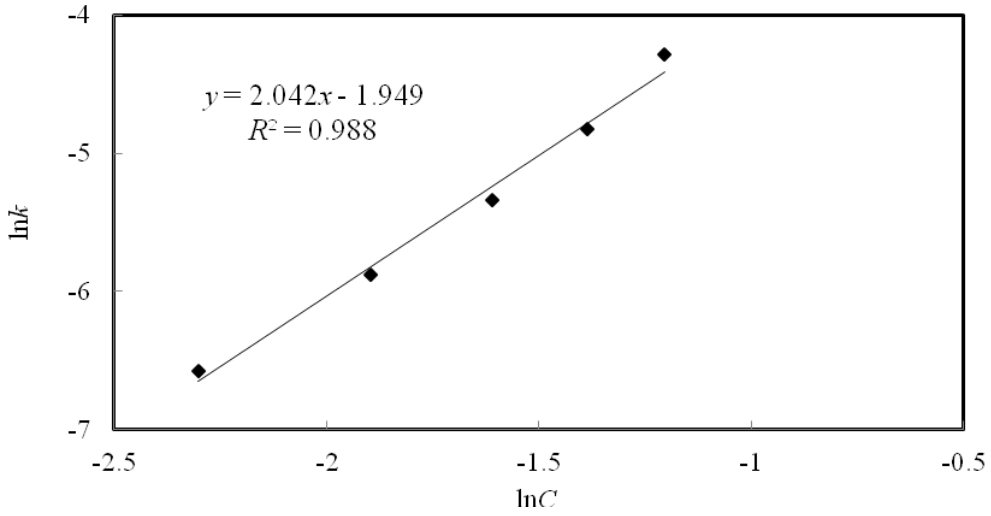

Fig. 16. Plot of ln *k* versus SSA concentration.

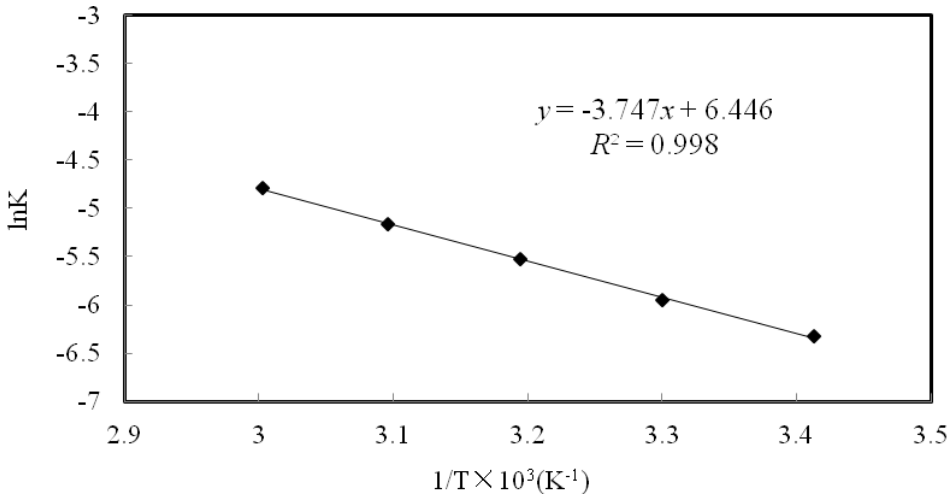

Fig. 17. Arrhenius plot of $1–3(1–x)^{2/3}+2(1–x)$ of the dissolution of cerussite.

Table 4 Apparent rate constants k_l, k_r, k_d, and k_m for the kinetic models and correlation coefficients.

Parameter	Diffusion through the liquid film		Surface chemical reaction		Diffusion through the product layer		Three dimensional diffusion model	
	X		$1-(1-x)^{1/3}$		$1-3(1-x)^{2/3}+2(1-x)$		$(1-(1-x)^{1/3})^2$	
	k_l (min^{-1})	R^2	k_r (min^{-1})	R^2	k_d (min^{-1})	R^2	k_m (min^{-1})	R^2
T (°C)								
20	0.0232	0.755	0.0097	0.859	0.0018	0.995	0.0021	0.995
30	0.0272	0.704	0.0120	0.847	0.0026	0.994	0.0033	0.994
40	0.0318	0.591	0.0152	0.816	0.0040	0.991	0.0052	0.992
50	0.0361	0.503	0.0189	0.808	0.0057	0.983	0.0080	0.995
60	0.0405	0.358	0.0243	0.823	0.0083	0.978	0.0133	0.993
C (mol/L)								
0.10	0.0196	0.799	0.0078	0.870	0.0012	0.993	0.0014	0.994
0.15	0.0257	0.641	0.0111	0.790	0.0023	0.989	0.0028	0.995
0.20	0.0311	0.580	0.0146	0.789	0.0037	0.983	0.0048	0.995
0.25	0.0361	0.503	0.0189	0.808	0.0057	0.983	0.0080	0.995
0.30	0.0407	0.389	0.0247	0.853	0.0085	0.989	0.0138	0.993
P (μm)								
320	0.0131	0.809	0.0049	0.855	0.0005	0.994	0.0005	0.994
200	0.0182	0.759	0.0072	0.841	0.0010	0.995	0.0012	0.993
124	0.0266	0.718	0.0117	0.856	0.0025	0.994	0.0031	0.992
80	0.0361	0.503	0.0189	0.808	0.0057	0.983	0.0080	0.995
50	0.0423	0.243	0.0277	0.831	0.0098	0.973	0.0174	0.991
S (rpm)								
200	0.0149	0.769	0.0056	0.828	0.0007	0.994	0.0007	0.995
400	0.0215	0.675	0.0088	0.788	0.0015	0.990	0.0017	0.995
600	0.0286	0.629	0.0129	0.805	0.0030	0.986	0.0037	0.991
800	0.0361	0.503	0.0189	0.808	0.0057	0.983	0.0080	0.995
1000	0.0414	0.365	0.0260	0.861	0.0091	0.987	0.0154	0.994

4 Conclusions

This study aimed to investigate the leaching kinetics of cerussite in SSA solution and the factors affecting leaching. The following conclusions were drawn based on the results.

(1) XRD and morphology studies on leaching residues indicated that a stable complex may be formed by a complexation reaction between SSA and lead ions.

(2) The leaching rate was determined to increase with increased stirring speed, solution temperature, and SSA concentration; as well as with decreased particle size. SSA was also clearly able to easily dissolve lead in cerussite.

(3) The optimum leaching conditions were determined to be 1000 rpm stirring speed, 60 °C reaction temperature, 50 μm particle size, and 0.3 mol/L SSA. The sufficient time to achieve over 95% lead extraction was 30 min.

(4) The leaching kinetics of cerussite in SSA solution was found to be controlled by the shrinking core model for the mixed kinetic model. E_a was calculated to be 37.07 kJ/mol at 20 °C to 60 °C.

(5) The leaching rate can be expressed as follows: $[1 - (1 - x)^{1/3}]^2 = [k_0(\mathrm{SS})^{6.852}(r_0)^{-1.943}(C)^{2.042}\exp(-37.07/RT)]t$. The orders of reaction with respect to stirring speed, particle size, and SSA concentration were found to be 6.852, −1.943, and 2.042, respectively.

Acknowledgements

This research project was supported by the National Natural Science Foundation of

China (51404119 & 51464029).

References

1 Z.H. Wu, D.B. Dreisinger, H. Urch and S. Fassbender, *Hydrometallurgy*, 2014, 142, 23–35.

2 A.A. Baba and F.A. Adekola, *J. Saudi. Chem. Soc*., 2012, 16, 377–386.

3 R.Z. Gutiérrez and G.T. Lapidus, *Hydrometallurgy*, 2014, 144–145, 124–128.

4 I. P. Pozdnyakov, V. F. Plyusnin, V. P. Grivin, D. Y. Vorobyev, A. I. Kruppa and H. Lemmetyinen, *J. Photoch. Photobio. A*., 2004, 162, 153–162.

5 J. Zhang, Q. S. Yan, J. P. Liu, T. Salmi, X. H. Lu and Y. S. Zhu, *J. Lumin.*, 2013, 134, 747–753.

6 P. Yin, Q. Xu, R. J. Qu and G. F. Zhao, *J. Hazard. Mater*., 2009, 169, 228–232.

7 S. R. Fan and L. G. Zhu, *J. Mol. Struct.*, 2007, 827, 188–194.

8 C.Y. Wen, *Ind. Eng. Chem*., 1968, 60, 34–54.

9 N. Demirklran, *Chem. Eng. J*., 2008, 141, 180–186.

10 N. Habbache, N. Alane, S. Djerad and L. Tifouti, *Chem. Eng. J.*, 2009, 152, 503–508.

11 A. Künkül, A. Gülezgin and N. Demirkiran, *Chem. Ind. Chem. Eng. Q.*, 2013, 19, 25–35.

12 C. F. Dickinson and G. R. Heal, *Thermochim. Acta.*, 1999, 340–341, 89–103.